Hydrogen storage in FeTi hydrides for stationary applications : material characterization and tank thermomechanical modeling

G. Gay, D. Chapelle, C. Lexcellent, D. Perreux, F. Thiebaud

Institut FEMTO-ST, UMR6174, 24 rue de l'Epitaphe 25000 Besançon, guillaume.gay@femto-st.fr

ABSTRACT:

This work is dedicated to H_2 storage in metal hydride $Fe_{1-x}Ti_1Mn_x$, for energy storage in autonomous radio relay stations, in the frame of FUI project "RHYTA" involving partnership with EADS Cassidian and Mahytec. The choice of this alloy is motivated by its trade-off in terms of fabrication costs (abundant raw material), ease of activation, equilibrium pressure (2.5 bars @25°C) and capacity (1.5% weight).

First, we will present characterization of the powder with granulometry measurements, PCI curves, and H_2 outflow capability (Fig.1).

Then, the presentation will focus on thermomechanical modeling of a hydride storage tank. Starting from a model developed in [1], we added the poromechanics behaviour of the powder described in [2] in order to assess the powder swelling during hydrogen absorption. This model implemented in COMSOL allows for dimensioning the H_2 tank (Fig.2) in order to optimize (i) thermal transfer and (ii) mechanical stress applied on the tank wall during charging/discharging of H_2.

KEYWORDS: Hydrogen, energy storage, hydrides, poromechanics

femto-st sciences & technologies
UFC Université de Franche-Comté
MaHyTec
CASSIDIAN AN EADS COMPANY
l'Europe s'engage en Franche-Comté avec le Fonds européen de Développement Régional
UNION EUROPEENNE

I) INTRODUCTION :

In the frame of FUI project "RHYTA" involving CASSIDIAN (EADS), MAHYTEC and UFC (University of Franche Comte), we develop hydrogen storage solutions based on solid hydrides. The aim is to provide hydrogen tanks dedicated to the storage of energy produced by solar panels inside an autonomous radio relay station. Those stations should be robust, easily installed, and highly reliable even in hostile environment. For this stationary application, hydrogen storage in FeTi metal hydrides is a good solution in terms of thermodynamics characteristics (temperature between -20°C and 50°C, equilibrium pressure between 1 and 10 bars), safety (low pressure), costs (no rare earth elements) and reliability. Before developing a thermodynamical model about the solid hydrogen storage in a tank, attention will be paid to FeTi hydride synthesis and characterization.

II) HYDRIDE SYNTHESIS AND CHARACTERIZATION

Hydride synthesis

It was demonstrated that FeTi needs to be activated thanks to a high temperature annealing (T>670K) before being able to absorb hydrogen [2]. This thermal treatment cracks the surface oxide, opening the path to hydrogen diffusion in the hydride bulk. However, this process has a cost and an other technique is preferred which consists in adding a third element, manganese (Mn), in the alloy composition. It was proven that manganese provides easier FeTi activation because (i) sub-oxides on the hydride surface are more permeable to hydrogen (ii) Ti_yMn_{1-y} aggregates are formed on the surface, creating a window for hydrogen penetration inside the hydride [3].

Fe_xTiMn_{1-x} hydrides are synthesized by induction heating fusion in a 5kg capacity furnace, followed by cooling under vacuum. The hydride composition is measured by X-ray fluorescence directly on the hydride blocks at the exit of the furnace with a handheld analyzer to check composition and uniformity of the alloy. Then, the hydride blocks are transformed in a coarsed-grained powder with a crusher blade. 100g of this powder is then poured into a small cylindrical test tank (height: 13cms, radius: 2.5cms) dedicated to hydrogen absorption and desorption measurements. The first step is the activation of the hydride which is done by applying multiple cycles of pressurization at P=35bars and T=0°C, followed by vacuum and heating at 65°C. In the case of $Fe_{0.85}Mn_{0.15}$, hydride starts to absorb after 3 cycles, and reaches the full absorption capacity after 8 cycles. On SEM (scanning electron microscopy) images made on activated powder (Figure 1-a), cracking of hydride grains is observed, leading to a decrease of their sizes. This decrease in grain size is characterized with a laser scattering particle distribution analyzer (Horiba partica LA-950V2). On Figure 1-b, grain size distribution is represented for different number of absorption/desorption cycles. We clearly observe a decrease in the diameter, starting from a coarsed-grain powder (Dmean =386 µm) to a fined-grained powder (Dmean = 60 µm).

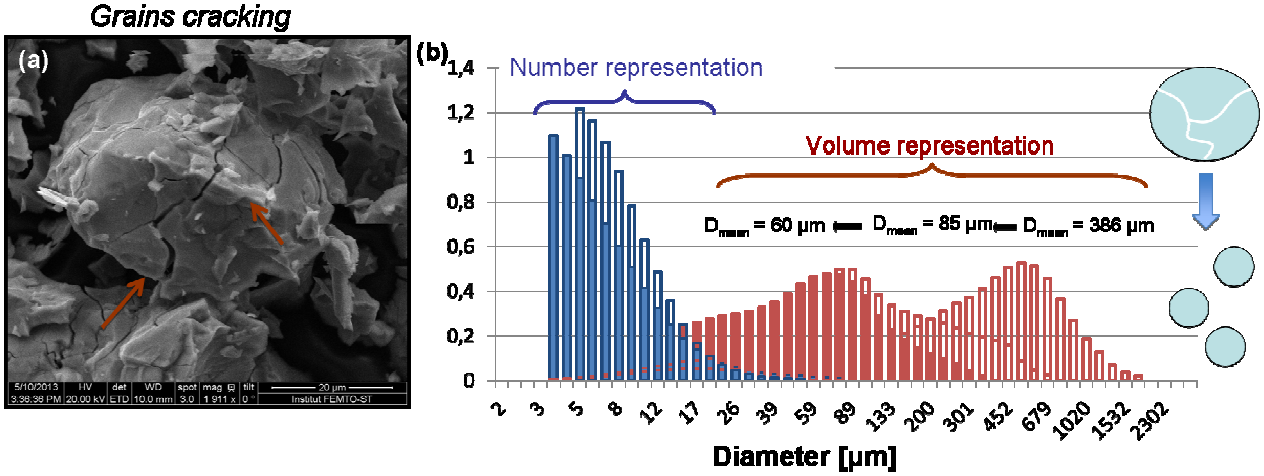

Figure 1 : (a) SEM observation of a $Fe_{0.85}TiMn_{0.15}$ hydride grain after activation **(b)** Granularity of $Fe_{0.85}TiMn_{0.15}$ hydride powder for increasing number of absorption/desorption cycles. Distributions based on grain volume and grain number are represented.

III) ABSORPTION/DESORPTION PROPERTIES OF SNTHEZISED HYDRIDES

Pressure-composition isotherms

Isothermal pressure-composition (PCI) of $Fe_{0.90}TiMn_{0.10}$ are plotted on Figure 2-a. Those curves give the equilibrium pressure of the hydride as a function of the mass of stored hydride (expressed in percentage of alloy mass). A tilted "plateau" is observed because of the phase transformation during hydrogen absorption. As expected by the Van't Hoff law [4], higher is the temperature, higher is the equilibrium pressure. Moreover, as can be seen on Figure 2-b, the reversible capacity of the hydride (quantity of hydrogen that can be released at atmosphere pressure) is decreasing at higher temperature because of the plateau narrowing.

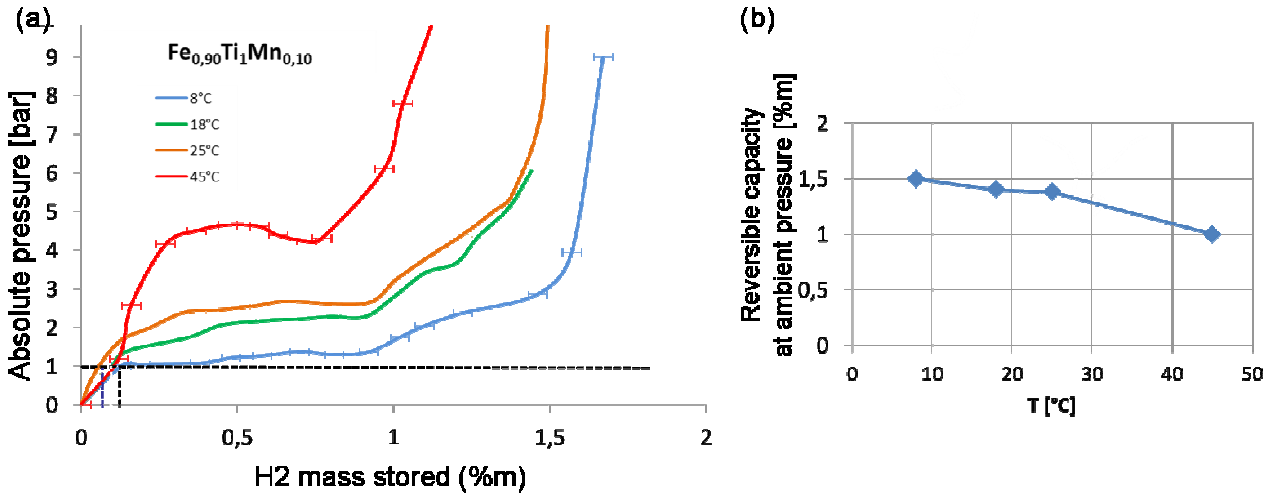

Figure 2 : (a) Isotherm Pressure-composition curve of $Fe_{0.90}TiMn_{0.10}$ at different temperatures **(b)** Plot of the reversible capacity at ambient pressure (1 ar) as a function of temperature, based on data of the PCI curves.

Hydrogen flow measurements

Hydrogen outflow from the hydride is measured with a gas flow controller (Brooks GF040). Temperature outside the tank is measured during desorption. Results obtained on 100g of $Fe_{0.90}TiMn_{0.10}$ are plotted on Figure 3-a, with a command flow of 50sccm (standard cm^3 per minute). In these conditions, the hydride tank is able to deliver 50 sccm during $1{,}3.10^4$ s, which corresponds to 1g of hydrogen. At this time, the temperature at the tank surface has decreased to 11 °C, and there are still around 0.4g of hydrogen that has not been delivered. The 50 sccm flow cannot be sustained anymore because the equilibrium pressure of the hydride at this low temperature is too close to the atmospheric pressure (1 bar). A solution to be able to deliver the full capacity of the tank at the expected flow (50 sccms) would be to heat the tank in order to maintain the hydride at constant temperature. Other tests at different imposed outflow were made and are synthesized on Figure 3-b. Obviously, larger is the flow, smaller is the desorption time capability. For the sake of comparison, tests were also made on $LaNi_5$ in the same experimental conditions. One observes that the two curves are similar.

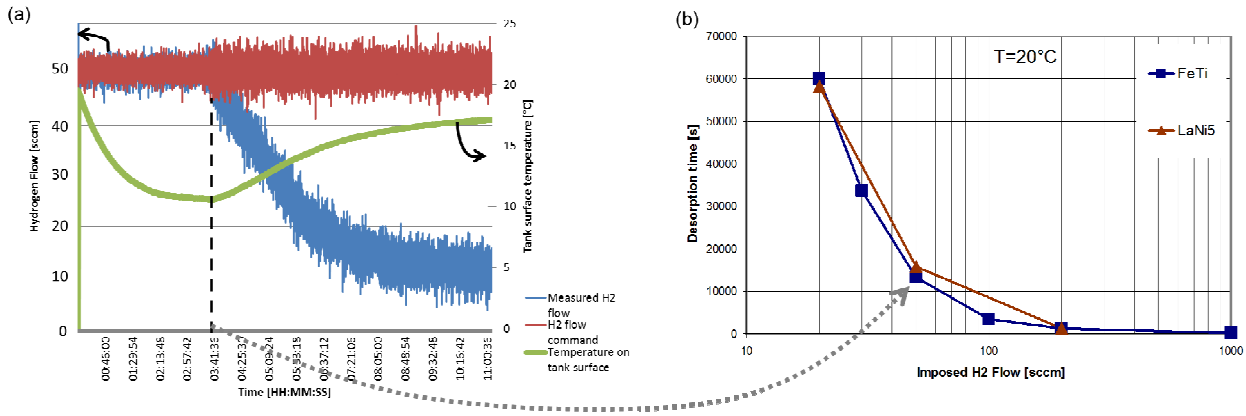

Figure 3 : (a) Plot of hydrogen outflow from a tank filled with $Fe_{0.9}TiMn_{0.1}$ at an external temperature of 20°C. **(b)** Plot of the maximal desorption time that can be sustained by a $Fe_{0.9}TiMn_{0.1}$ tank as a function of imposed H_2 flow.

IV) THERMOMECHANICAL MODELING OF THE HYDROGEN TANK

4.1) Context

Many studies proposed to model the behavior of hydrogen storage in metal hydride reactors, each model being original in the fact that they consider different hypothesis on the description of physical phenomena [5][6][7][8][9][10]. Basically, a large majority of models models take into those four main phenomena :

• *Kinetics of reaction* which describes the rate of reaction as a function of thermodynamics data such as temperature, hydrogen pressure, hydrogen concentration stored in the hydride.

• *Equilibrium pressure* which is a thermodynamics law linking the equilibrium pressure of hydrogen in the gas phase to the temperature and hydrogen concentration.

• *Energy conservation* : this thermodynamics equation is describing the heat generation and transfer through the reactor.

• Mass conservation : this equation describes hydrogen flow in the reactor. A. Chaise et al. [11] have defined a criterion that allows to discriminate situations for which hydrogen flow in the hydride can be neglected. Indeed, in some cases, the hydrogen pressure in the gas phase can be considered as uniform in the tank, mass conservation equation thus becoming useless.

An other interesting phenomenon is the mechanical behaviour of the powder. While some experimental works has demonstrated the large swelling of hydrides and its impact on tank walls [12] [13][14][15][16], not much work has been done to model it [hu2011mechanism]. In the present model, we propose to take into account the mechanics of the hydride with a continuum approach, based on the theory of poromechanics largely described by O.Cousy [17].

4.2) Model hypothesis

Hydrogen gas is absorbed in a metal hydrid which constitutes the getter material. Associated to the hydrogen absorption increase, the solid solution α can be the seat of a phase transition towards an hydrid one called β as described in [18].
In order to solve the problem, i.e. the tank filling, some hypothesis to simplify the problem are necessary:

1. the mechanical behavior of the solid phase is considered as the one of an isotropic elastic body (if one take into account the swelling due to H atoms absorption ,a superelastic behavior can be stated). The hydride powder media is considered as a continuum material.

2. the solid behavior is considered as reversible at the thermodynamical point of view

3. the small deformation hypothesis is stated

4. the gas kinetic energy is not taken into account in the energy balance equation

4.3) Model description

To solve the problem, we must compute the four unknows which are the pressure of H_2 in the tank (p), the temperature (T), the concentration of hydrogen absorbed by the hydride (c), the mechanical displacement vector ($\vec{\xi}$). The detailed description of the model is not the aim of this paper, it will be further detailed in an other paper published elsewhere. However, for the sake of reader information a summary of the main equations is described :

1. Conservation of hydrogen moles and gas diffusion equation (darcy's law) are compiled into:

$$\frac{d}{dt}\left(\frac{\phi p}{RT}\right)+\frac{dc}{dt}=\nabla\cdot\left(\frac{\kappa}{\eta}\nabla p\right) \qquad \text{Equation 1}$$

With Φ the porosity, R the perfect gas constant, κ the hydride permeability and η the dynamic viscosity of hydrogen.

2. Energy conservation equation, also called thermal equation:

$$T\left(\frac{dS}{dt}+\nabla\cdot(s_G\overrightarrow{u_G})\right)=-\nabla\cdot\vec{q}+\phi_G \qquad \text{Equation 2}$$

With S the entropy density of the porous system (gas and hydride grains), s_G the gas molar entropy, $\overrightarrow{u_G}$ the gas molar flux vector, $\vec{q}=-\lambda\nabla T$ the heat flow vector (λ being the thermal conductivity of the system), Φ_G the dissipation related to the gas mass transfer which can be expressed as a function of main unknows.

3. Reaction kinetics equation

For the sake of numerical implementation simplification, we chose to use one single reaction kinetics for the whole three domains of the PCI curve (α, α+β and β):

$$\frac{dc}{dt}=C_a\exp\left(-\frac{E_a}{RT}\right)\ln\left(\frac{p}{p_{eq}}\right) \qquad \text{Equation 3}$$

With C_a and E_a material constants and p_{eq} the equilibrium pressure of the hydride depending on T anfd c and calculated with the Pons formula [19].

4. Navier equation of displacements

Strain tensor is expressed as a function of hydrostatic and deviatoric components

$\varepsilon_{ij}=e_{ij}-\frac{1}{3}\varepsilon\delta_{ij}$ with ε the volumetric dilatation and *sij* the deviatoric strain.

Similarly, stress tensor is decomposed in :

$\sigma_{ij}=s_{ij}+\sigma\delta_{ij}$ with σ the hydrostatic stress and *sij* the deviatoric stress.

In the case of linear isotropic elasticity, state equation of the poroelastics solid leads to the following system of equations [17]:

$$\begin{aligned}\sigma&=K(\varepsilon-3\alpha_S(T-T_0)-\alpha_G c)-bp\\ s_{ij}&=2\mu e_{ij}\end{aligned} \qquad \text{Equation 4}$$

μ is the shear modulus, α_S is the thermal dilatation of the solid matrix, α_G is a dilatation coefficient aiming to take into account the swelling of the hydride grains during hydrogen absorption, K is the elastic modulus of the hydride, b is the Biot coefficient corresponding to the fraction of the volumetric dilatation due to the porosity variation.

In the absence of body forces, the momentum equation is $\nabla\cdot\underline{\sigma}=0$. Using strain/displacement relation in the frame of small deformation and reporting expression of stress tensor (Equation 4) allows for obtaining the so-called Navier equation :

$$(K+\frac{1}{3})\nabla(\nabla\cdot\vec{\xi})+\mu\Delta\vec{\xi}-b\nabla p-3\alpha_S K\nabla T-K\alpha_G\nabla c=0 \qquad \text{Equation 5}$$

4.4) Implementation in COMSOL and results

The model described in the previous paragraph has been implemented in COMSOL Multiphysics. We will present the results obtained on two geometries. The first one is a axisymmetric tank (height 130 mm and radius 50 mm). The imposed boundary conditions are summarized in Figure 4-left. On the top of the hydride, we apply a constant pressure of hydrogen (P_{H2} = 5 bar). On the tank walls, a transfer coefficient of 3000 $W.m^{-2}$ is chosen. The mechanical boundary condition is a contact between the hydride powder and the aluminium tank wall at r=R and z=0, while the top surface at z=H is free. In the results presented here, we consider the displacements of the tank walls equal the displacements of the powder, which does not has a real physical meaning since the powder should slide along the wall, thus decreasing the radial constraints applied by the powder on the wall.

We represent on Figure 4-right the temperature, quantity of hydrogen stored in the hydride and pressure after 10^3 seconds of charging. As expected, the concentration of hydrogen in the hydride is larger on the border of the tank because the heat evacuation is more efficient there, as observed on the temperature plot. The pressure is not uniform in the powder, and we observe a 1 bar pressure difference between the top and the bottom of the tank. This pressure loss is due to the small particle diameter considered in the model (10 µm) and the relative dense medium with an initial porosity of 0.2.

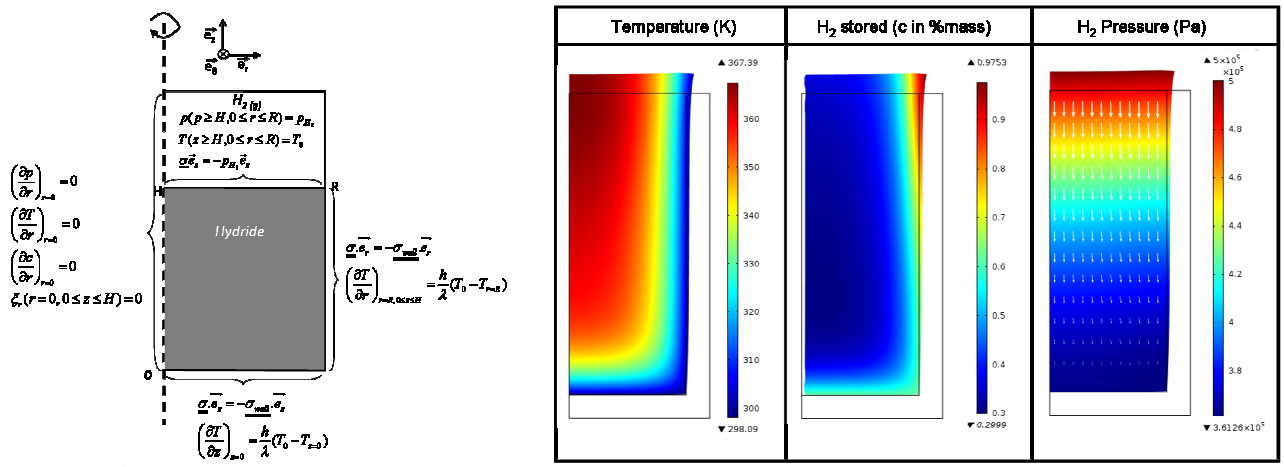

Figure 4 : (left) Boundary conditions on the axisymmetric hydride tank. The aluminium tank wall is not represented on this picture, but the two walls should be in contact with the hydride at r=R and z=0. **(right)** Representation of temperature, concentration of hydrogen stored and H_2 pressure in the tank after 10^3 seconds charging with fixed pressure at the top of the tank (P=5bar). White arrows on the right represent the hydrogen speed vector ($\overrightarrow{u_G}$). The geometry of the tank is deformed because of the thermal dilatation and the swelling due to hydrogen absorption in hydride grains.

Concerning the mechanical behaviour of the tank, radial stress in the hydride ($\underline{\underline{\sigma}} \cdot \overrightarrow{e_r} \cdot \overrightarrow{e_r}$) and in the tank walls are represented on Figure 5, with the deformation of the geometry multiplied by a factor 30. In this simulation, a powder swelling of 1% is considered at the end of the absorption. More specifically, the radial stress along a cut line in the radial direction (Figure 5-a) and in the axial direction (Figure 5-b) in the hydride powder are represented on the graph.

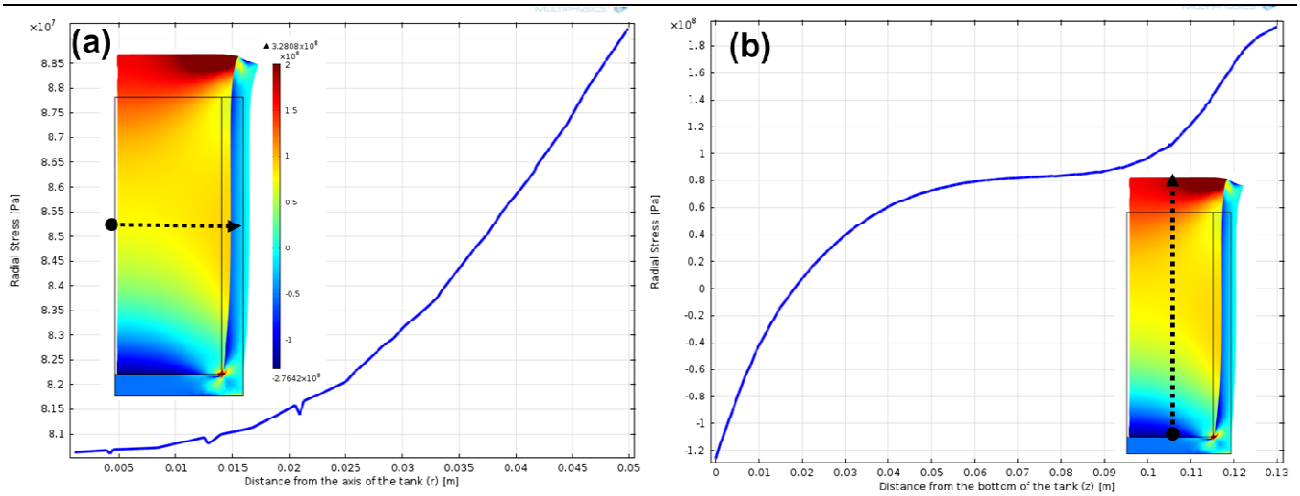

Figure 5 : Graphics representing the radial stress in the hydride and in the tank wall at the final state, when the hydride is fully charged by hydrogen. The insets show the deformed geometry multiplied by a factor 30 **(a)** radial stress along a cut line at z=7 cms **(b)** radial stress along a cut line at r=3 cms

The second tank geometry is a more complex one, and is dedicated to be used in the project demonstrator. This is a cylindrical tank filled with hydride. In order to enhance the heat exchange with the atmosphere, a helicoïdal tube heat exchanger with water circulation is inserted in the tank. Experimental measurements on this tank have shown that the temperature increase between entrance and outside of the heat exchanger is around 2°C. Consequently, temperature of the water inside the tube is considered constant in the simulation, which is reducing the computing time. Hydrogen concentration in the hydride after 1000s charging at a pressure of 5 bars is represented on Figure 6.

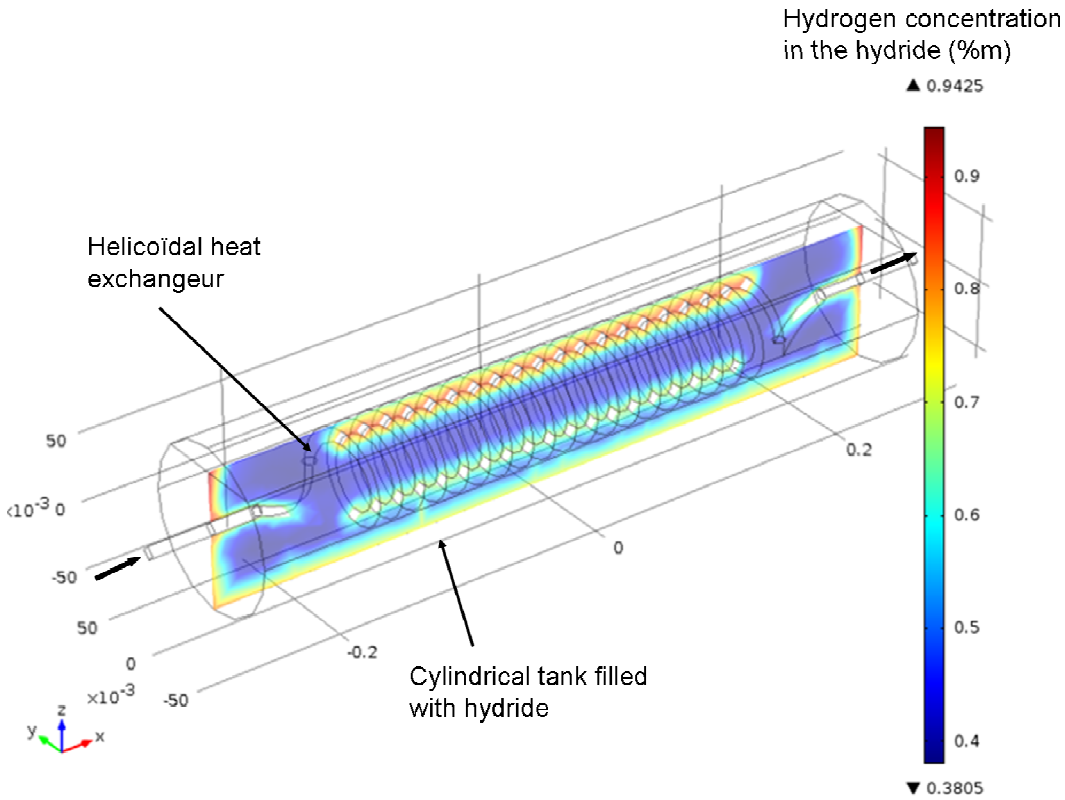

Figure 6 : H_2 concentration in a cylindrical hydride tank filled with FeTi after 1000s. A helicoïdal fluid circulation system enables faster cooling of the hydride.

Conclusion and perspectives

In this paper, we have presented Fe_xTiMn_{1-x} alloys synthesized in our lab in terms of granularity, PCI curves and hydrogen flow capability. Then, we've presented preliminary results of the thermomechanical modeling of the hydride tank that will be used in the autonomous relay station for the RHYTA project. Perspectives of this work include finer characterization of the hydride tank, especially on the thermal aspect. Indeed, calibration of the thermomechanical model needs to be done (hydride conductivity, reaction kinetics, strain…) so as it can be used in the future to design hydride tanks geometry for optimized heat transfer and mechanical resistance to hydride swelling.

References (Arial font, 10-point):

[1] G. Gondor and C. Lexcellent, "Analysis of hydrogen storage in metal hydride tanks introducing an induced phase transformation," *Int. J. Hydrog. Energy*, vol. 34, no. 14, pp. 5716–5725, Jul. 2009.

[2] L. Schlapbach and T. Riesterer, "The activation of FeTi for hydrogen absorption," *Appl. Phys. Solids Surf.*, vol. 32, no. 4, pp. 169–182, Dec. 1983.

[3] Y. Shenzhong, Y. Rong, H. Tiesheng, Z. Shilong, and C. Bingzhao, "A study of the activation of FeTi and Fe0.9 TiMn0.1," *Int. J. Hydrog. Energy*, vol. 13, no. 7, pp. 433–437, 1988.

[4] L. Schlapbach and A. Züttel, "Hydrogen-storage materials for mobile applications," *Nature*, vol. 414, no. 6861, pp. 353–358, Nov. 2001.

[5] P. Marty, J.-F. Fourmigue, P. D. Rango, D. Fruchart, and J. Charbonnier, "Numerical simulation of heat and mass transfer during the absorption of hydrogen in a magnesium hydride," *Energy Convers. Manag.*, vol. 47, no. 20, pp. 3632–3643, Dec. 2006.

[6] A. Demircan, M. Demiralp, Y. Kaplan, M. D. Mat, and T. N. Veziroglu, "Experimental and theoretical analysis of hydrogen absorption in – reactors," *Int. J. Hydrog. Energy*, vol. 30, no. 13–14, pp. 1437–1446, Oct. 2005.

[7] S. B. Nasrallah and A. Jemni, "Heat and mass transfer models in metal-hydrogen reactor," *Int. J. Hydrog. Energy*, vol. 22, no. 1, pp. 67–76, Jan. 1997.

[8] T. Nakagawa, A. Inomata, H. Aoki, and T. Miura, "Numerical analysis of heat and mass transfer characteristics in the metal hydride bed," *Int. J. Hydrog. Energy*, vol. 25, no. 4, pp. 339–350, Apr. 2000.

[9] M. Gambini, M. Manno, and M. Vellini, "Numerical analysis and performance assessment of metal hydride-based hydrogen storage systems," *Int. J. Hydrog. Energy*, vol. 33, no. 21, pp. 6178–6187, Nov. 2008.

[10] K. B. Minko, V. I. Artemov, and G. G. Yan'kov, "Numerical simulation of sorption/desorption processes in metal-hydride systems for hydrogen storage and purification. Part I: Development of a mathematical model," *Int. J. Heat Mass Transf.*, vol. 68, pp. 683–692, Jan. 2014.

[11] A. Chaise, P. Marty, P. de Rango, and D. Fruchart, "A simple criterion for estimating the effect of pressure gradients during hydrogen absorption in a hydride reactor," *Int. J. Heat Mass Transf.*, vol. 52, no. 19–20, pp. 4564–4572, Sep. 2009.

[12] B. Y. Ao, S. X. Chen, and G. Q. Jiang, "A study on wall stresses induced by LaNi5 alloy hydrogen absorption–desorption cycles," *J. Alloys Compd.*, vol. 390, no. 1–2, pp. 122–126, Mar. 2005.

[13] B. Charlas, A. Chaise, O. Gillia, P. Doremus, and D. Imbault, "Investigation of hydride powder bed swelling and shrinking during hydrogen absorption/desorption cycles under different compressive stresses," *J. Alloys Compd.*, vol. 580, Supplement 1, pp. S149–S152, Dec. 2013.

[14] F. Qin, J. Chen, and Z. Chen, "The hydriding–dehydriding characteristics of La0.6Y0.4Ni4.8Mn0.2 and their influences in the surface strain on small-scale, thin-wall and vertical containers," *Mater. Des.*, vol. 29, no. 10, pp. 1926–1933, Dec. 2008.

[15] K. Nasako, Y. Ito, N. Hiro, and M. Osumi, "Stress on a reaction vessel by the swelling of a hydrogen absorbing alloy," *J. Alloys Compd.*, vol. 264, no. 1–2, pp. 271–276, Jan. 1998.

[16] B. Charlas, A. Chaise, O. Gillia, P. Doremus, and D. Imbault, "Investigation of hydride powder bed swelling and shrinking during hydrogen absorption/desorption cycles under different compressive stresses," *J. Alloys Compd.*

[17] O. Coussy, *Mechanics and Physics of Porous Solids*. Wiley, 2010.

[18] C. Lexcellent and G. Gondor, "Analysis of hydride formation for hydrogen storage: Pressure–composition isotherm curves modeling," *Intermetallics*, vol. 15, no. 7, pp. 934–944, Jul. 2007.

[19] M. Pons and P. Dantzer, "Determination of thermal conductivity and wall heat transfer coefficient of hydrogen storage materials," *Int. J. Hydrog. Energy*, vol. 19, no. 7, pp. 611–616, Jul. 1994.